ISSN (Online) 2321 – 2004
ISSN (Print) 2321 – 5526

INTERNATIONAL JOURNAL OF INNOVATIVE RESEARCH IN ELECTRICAL, ELECTRONICS, INSTRUMENTATION AND CONTROL ENGINEERING
Vol. 2, Issue 8, August 2014

Fuzzy Ruler Based Energy Management System for Hybrid Battery -Ultra Capacitor DC Micro Grid System

Jarina Begum[1], CH.Sampath Kumar[2], Shaik Khamuruddin[3]

M.Tech, Control Systems, ARTI, Warangal, India[1]

Associate Professor (EEE), Project Coordinator of M.Tech ARTI, Warangal, India[2]

Associate Professor (EEE), Head of EEE Department, ARTI, Warangal, India[3]

Abstract:-This paper represents implementation of an alloyed battery–ultra capacitor energy management system (EMS) by using fuzzy controllers, analysis and evolution of better battery power management systems is proposed in this paper, added advantage of ultra capacitor will gives optimal storage charging and discharging characteristics, also improves the life cycle energy storage devices .discharging current and state of charge (SOC%) of battery storage system is shown by MATLAB/SIMULINK. Proposed DC micro grid system is designed and analyzing results are shown.

Key words: Dc microgrid, battery energy management, fuzzy controller, Ultra capacitor, Fuzzy logic

I. INTRODUCTION

DC microgrids is attracting growingly attention because of the advantage of eliminating long distance transmission and in distribution lines of inherent capacity with easily integrating energy storage, alternative power sources. This shows the interest of innovative transportation systems with clean and pure renewable energy sources as per replacement for fossil-fuel based vehicles. In such systems, the fuel cell stacks, battery banks, and super capacitor banks are usually clean energy sources. The FC and BAT are energy sources those directly converts the chemical energy reaction to the electrical energy. However, there are some known technical limitations to Fuell cells. they are having low efficiency in low load demand, slow power transfer rate in transition situations, and a much cost per watt.. In comparison with batteries and Fuell cells, super capacitors shows a high power density but a low energy density.

Eventually, a combination of a primary energy source such as an Fuel Cells and more than one secondary energy sources such as super capacitors and batteries, is usually used in electric vehicles to satisfy different energy requirements (see Figure 1). In this combination, the primary energy sources and the secondary energy sources are sized for the continuous, transient energy requirements. The primary energy sources can be sized to the average energy and not to the peak of the energy demand. In this proposed sytsem, a DC microgrid consists a fuel cell, a battery, and a super capacitor is studied.

There are three main architectures with energy management strategies are detailed. The emphasis is put on control and an impact on the power architecture on control strategies. A simulation will be developed, detailed and Transient and steady state behavior of system will studied by simulations. Three operating modes ie., normal, overload and regeneration mode will be in consideration.

Interactive GUI animation will be performed using a simulation program and a giving driving cycle containing above operating modes. These interactive simulations are allowed users evaluating impact of the energy management and the power control on the efficiency of DC microgrid.

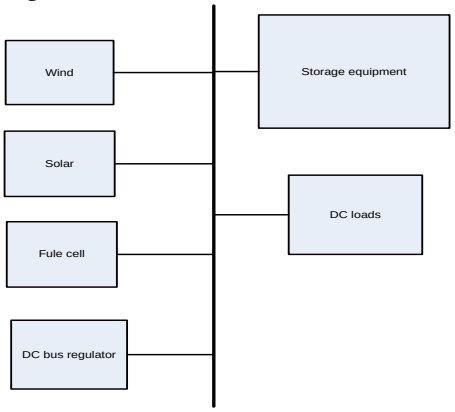

Fig.1 schematic diagram of proposed microgid systems

II. MICROGRID COMPONENTS

In this proposed system is to analize microgrid system here solar panel arrays, wind power generation and fuel cell ,the modelling of micro grid input component using Matlab/simulink ,designed on according to specifications of proposed microgrid systesm .

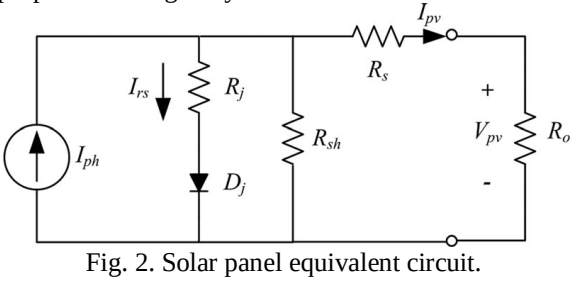

Fig. 2. Solar panel equivalent circuit.

ISSN (Online) 2321 – 2004
ISSN (Print) 2321 – 5526

INTERNATIONAL JOURNAL OF INNOVATIVE RESEARCH IN ELECTRICAL, ELECTRONICS, INSTRUMENTATION AND CONTROL ENGINEERING
Vol. 2, Issue 8, August 2014

a) Modeling of Solar Cell

The equivalent circuit of solar panel is shown in Fig. 2. Solar panel current equation is expressed by (1)-(3)

$$I_{pv} = n_p I_{ph} - n_p I_{rs}\left[\exp\left(\frac{q}{KTA}\frac{V_{PV}}{n_s}\right) - 1\right] \quad (1)$$

where *V*pv is solar panels output voltage , *I*pv is solar panels output current, *ns* is no.of solar panels in series, *np* is no. of solar panels in parallel, *k* is Boltzmann constant (1.38 × 10−23 J/K), *q* is one electron charge (1.6 × 10−19C), *A* is ideality factor (1–2), *T* is the surface temperature of the solar panels (K), and *Irs* as reverse saturation current. The characteristic is reverse saturation current *Irs* varies with temperature, as expressed in (2)

$$I_{rs} = I_{rr}\left[\frac{T}{T_r}\right]^3 \exp\left(\frac{qE_g}{kA}\left(\frac{1}{T_r} - \frac{1}{T}\right)\right) \quad (2)$$

where *Tr* is reference temperature of the solar panels (K), *I*rr is the reverse saturation current of the solar panels at temperature *Tr* (K), and *Eg* is energy band gap of the semiconductor material

$$I_{ph} = [I_{scr} + \alpha(T - T_r)]\frac{S}{100} \quad (3)$$

where *I*scr is the short-circuit current at reference temperature *Tr* and illumination intensity 1 kW/m2 , α is the short-circuit current temperature coefficient of solar panels, and *S*is illumination intensity (kW/m2). In this study used Sharp NUS0E3E solar modules, each one is a power rating of 180 W, as photovoltaic device of microgrid system.

This study used solar 5 kW power system, generated by 2 photovoltaic arrays in parallel, where each array was built with 14 solar panels in series. The simulation output power versus output voltage of the solar cells .This study is used constant illumination intensity 1 kW/m2 and a constant temperature with a varying *V*pv for simulation verification.

b) Wind Turbine Modeling

The power generated by wind turbine is expressed as

$$P_w = 0.5\rho A V^3 C_p(\lambda, \theta) \quad (4)$$

where *PW* is power generated by the wind turbine *W*, *P* is density of gas in the atmosphere (kg/m), *A* is cross-sectional area of a wind turbine blade m2 , *V* is wind velocity (m/sec), and *Cp* is the wind turbine energy conversion coefficient.

The density of gas ρ and energy conversion coefficient *CP* in (4) is expressed by (5) and (6), respectively

$$\rho = \left(\frac{353.05}{T}\right)\exp^{-0.034\left(\frac{Z}{T}\right)} \quad (5)$$

$$C_p(\lambda, \theta) = \left(\frac{116}{\lambda_i} - 0.4 * \theta - 5\right)\cdot 0.5\exp^{\frac{-16.5}{\lambda_i}} \quad (6)$$

where *Z* is the altitude, *T* is the atmospheric temperature, λi is the tip speed ratio, and θ is the blade tilt angle. Equation (7) gives the expression of the tip speed ratio λi in (6) and (8) is the expression of the initial tip speed ratio λ in (7)

$$\lambda_i = \frac{1}{1/(\lambda + 0.089\theta) - 0.035/(\theta^3 + 1)} \quad (7)$$

$$\lambda = r\frac{\omega}{V} \quad (8)$$

The wind turbine used in this studywasAWV-1500 of Gallant Precision Machining Company, Ltd. Wind speed is the most critical factor in wind power generation. This simulated output power *PW* of the wind turbine with various wind speeds *V*.

c) Lithium-Ion Battery Modeling

Eq. (9) is the discharge equation and (10) the charge equation of the lithium-ion battery

$$f_1(it\, i^*i) = E_0 - K\cdot\frac{Q}{Q - it}\cdot i^* - K\cdot\frac{Q}{Q - it}\cdot it + A\exp(-B.it) \quad (9)$$

$$f_2(it\, i^*i) = E_0 - K\cdot\frac{Q}{Q + 0.1\cdot Q}\cdot i^* - K\cdot\frac{Q}{Q - it}\cdot it + A\exp(-B.it) \quad (10)$$

where *E*0 is initial voltage (V), *K* is polarization resistance (Ω), $i*$ is low-frequency dynamic current (A), *i* is battery current (*A*), itis the battery extraction capacity (Ah), *Q* is maximum battery capacity (Ah), *A* is exponential voltage (V), *B* is exponential capacity (Ah)−1 .SOC of the battery is an important factor, which is calculated By

$$SOC = 100\left(1 - \frac{\int_0^t idt}{Q}\right) \quad (11)$$

This study simulated with constant discharge of 5 A for validation and observation of SOC variation.. The battery voltage is easy to measure and implement in the circuit. From the simulated results, we can see the nonlinearity between voltage and SOC of the Li-ion battery. Therefore, the SOC parameter of batteries has been selected as the design factor instead of battery voltage in this paper

d)Fuel Cell Modeling

Fuel cells provide a high efficiency clean alternative to today's power generation technologies. The polymer electrolyte membrane (PEM) fuel cell has gained some acceptance in medium power commercial applications such as creating backup power, grid tied distributed generation, and electric vehicles. The output voltage *E* of the PEM fuel cell is represented as

$$E = E_n - (-V_{act} + V_{ohm} + V_{con}) \quad (12)$$

where *En* is Nernst voltage, *V*act is the activation over potential, *V*ohm is ohmic over potential, and *V*con is concentration Over potential

$$V_{act} = -[\xi_1 + \xi_2\cdot T + \xi_3\cdot T\cdot\ln(Co_2) + \xi_4\cdot T\cdot\ln(i_f)] \quad (13)$$

$$V_{ohm} = i_f\cdot R_M \quad (14)$$

$$R_M = \frac{181.6[1 + 0.03(i_f/A_f) + 0.062(T/303)^2(i_f/A_f)^{2.5}]}{[\lambda_1 - 0.634 - 3(i_f/A_f)]\exp\left(4.18\left((T-303)/T\right)\right)}\cdot\frac{l_1}{A_f} \quad (15)$$

$$V_{con} = -B_0\cdot\ln\left(1 - \frac{J}{J_{max}}\right) \quad (16)$$

where *T* is operating absolute temperature, *C*o2 is concentration of oxygen, if is output current of the fuel cell, ξ1,2,3,4 are reference coefficients, *l*1 is effective thickness of membrane, λ1is adjustable coefficient, *Af* is effective area, *B*0 is operating constant, *J* is current density, and *J*max is maximum current density. The simulated output voltage with constant discharge of 10A

ISSN (Online) 2321 – 2004
ISSN (Print) 2321 – 5526

INTERNATIONAL JOURNAL OF INNOVATIVE RESEARCH IN ELECTRICAL, ELECTRONICS, INSTRUMENTATION AND CONTROL ENGINEERING
Vol. 2, Issue 8, August 2014

III. BATTERY AND ULTRA CAPACITOR

By combining chemistries of the ultra capacitor and the lithium-ion batteries, a company called Ioxus has created hybrid energy-storage device that can could recharge power tools in minutes and should never need to be replaced. The company said future incarnations could be used to capture energy from some braking vehicles.

Super capacitors capture and releases energy in seconds and can do in millions of times, but they can store only about 5 percent as much energy of lithium-ion batteries. The hybrid can store more than twice of energy by volume in standard ultra capacitor. That is still much less than one lithium-ion battery, but hybrid could be recharged quickly over 20,000 times of against few hundred cycles for a normal battery.

The hybrid energy storage device is consists of an etched aluminum film coated on one side with a carbon slurry, which is similar to electrode found in a ultra capacitor. The other electrode, on the other side of film, is coated not with carbon but with lithium-ion material, is providing more energy storage capacity. The film is wound into cylinder to make finished device.

IV. INTELLIGENT MANAGEMENT SYSTEM

As shown in Fig. 3, the system configuration of the proposed micro grid system includes five major blocks. To design an accurate controller of the proposed micro system, the dynamic mathematical models of the power sources (PV, wind turbine, and fuel cell), dc/dc converters (buck-boost, buck, and phase shifted full-bridge converters), bidirectional converter (symmetrical full-bridge converter), and bidirectional inverter (full bridge inverter) of the integrated micro-system are necessary.

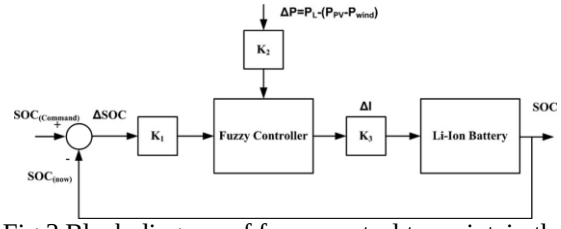

Fig.3 Block diagram of fuzzy control to maintain the desired SOC of the battery.

The fuzzy controller is applied in the proposed microgrid power supply system, as shown in Fig. 3. To obtain the desired SOC value, the fuzzy controller is designed to be in charging mode or discharging mode for the proposed microgrid system. The input variables of the fuzzy control are ΔSOC and Δ*P* and output variable is Δ*I*. The definition of input and output variables are listed as follows:

$$\Delta SOC = SOC_{command} - SOC_{now} \quad (17)$$

$$\Delta P = P_L - (P_{wind} + P_{pv}) \quad (18)$$

The power difference Δ*P* is between required power for load and the total generated power of the microgrid. The fuel cells only provide base power for the emergency loads when the system fails. Therefore, the fuel cell is not considered as power source.

TABLE I
FUZZY CONTROL RULES

ΔI		**ΔP**				
		NB	NS	ZO	PS	PB
ΔSOC	NB	PB	PB	PB	PB	PB
	NS	PB	PB	PS	PS	PB
	ZO	ZO	ZO	ZO	PS	PB
	PS	NS	NS	NS	NS	PB
	PB	NB	NB	NB	NB	PB

The generated power comes from solar power *P*pv, wind turbine *P*wind and power load *PL* for the proposed system. The input and output membership functions of fuzzy control contain five grades: NB (negative big), NS (negative small), ZO (zero), PS (positive small), and PB (positive big), as shown in Figs. 4 and 5.

By input scaling factors K1 and K2, we can determine the membership grade and substitute it into the fuzzy control rules to obtain the output current for charge and discharge variance Δ*I* of the Li-ion battery. If the Δ*P* is negative, it means that the renewable energy does not provide enough energy to the load.

Thus, the battery must operate in charging mode; if the ΔSOC is negative, it means that the SOC of the battery is greater than the demand SOC. Thus, the battery must operate in discharge mode.

The control rules of this study prioritize selling additional electricity generated by the renewable energy in response to the present control strategy of microgrid development for selling electricity and increasing. Table I shows the fuzzy rules of the proposed system.

For example, the output variable Δ*I* is PB (the degree of discharging current is large) when the input variable Δ*P* is NB (the amount of electricity to sell is large) and input variable ΔSOC is NS (greater than the SOC command and the membership degree is small).

However, the output variable Δ*I* is NS (the degree of charging current is small) when the input variable Δ*P* is NB (the amount of electricity to sell is large) and input variable ΔSOC is PS (smaller than the SOC command and the membership degree is small).

Table I shows the fuzzy rules of the proposed system. For example, the output variable Δ*I* is PB (the degree of discharging current is large) when the input variable Δ*P* is NB (the amount of electricity to sell is large) and input variable ΔSOC is NS (greater than the SOC command and the membership degree is small).

However, the output variable Δ*I* is NS (the degree of charging current is small) when the input variable Δ*P* is NB (the amount of electricity to sell is large) and input variable ΔSOC is PS (smaller than the SOC command and the membership degree is small).

ISSN (Online) 2321 – 2004
ISSN (Print) 2321 – 5526

INTERNATIONAL JOURNAL OF INNOVATIVE RESEARCH IN ELECTRICAL, ELECTRONICS, INSTRUMENTATION AND CONTROL ENGINEERING
Vol. 2, Issue 8, August 2014

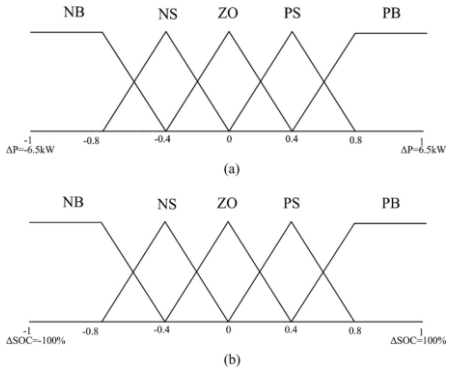

Fig. 4. Input membership functions of variables: (a) ΔP and (b) ΔSOC.

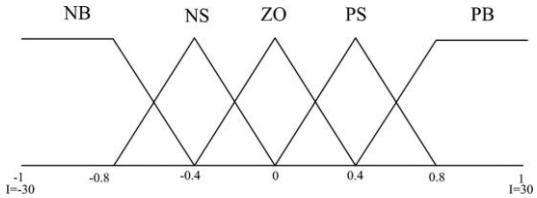

Fig. 5. Output membership function of variable ΔI

The output variable is NS instead of NB when the system is operated in the above conditions because selling electricity is the first priority in this case. Thus, the fuzzy control table of the proposed dc microgrid system is not symmetrical. To extend the life of storage batteries in the design of fuzzy control, the fuzzy control rules are set to maintain battery SOC above 50%. Moreover, in the fuzzy control rules the Li-ion battery is forced to discharge as the control strategy when power demand at load was greater than the power generated by the renewable energy.

V. SIMULATION RESULTS

As shown in fig 1 proposed system is analyzed using MATLAB .This model consists of consists of a 5 kW solar module, a 1.5 kW wind turbine module, a 1.5 kW Li-ion battery module, and a 6.5 kW load. The simulated output voltage with constant discharge of 10A is shown in Fig. 6. This AWV-1500 of Gallant Precision Machining Company, Ltd. simulated output power *PW* of the wind turbine with various wind speeds *V* is shown in Fig. 7 The simulated output power versus output voltage of the solar cell is shown in Fig. 8. This study used constant illumination intensity 1 kW/m2andconstant temperature with varying *V*pv for simulation verification..

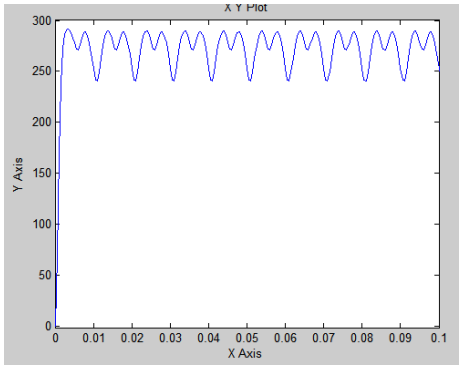

Fig.6 Simulated voltage of the fuel cell with a constant discharge of 10 A

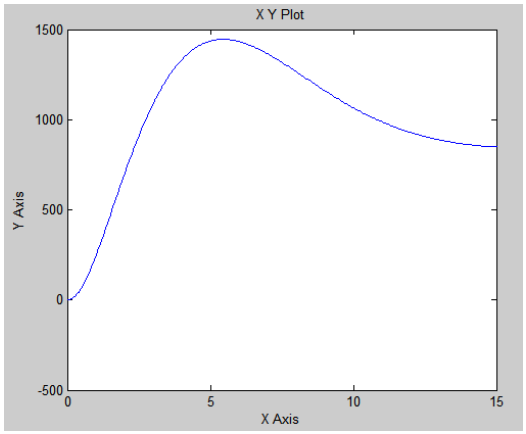

Fig. 7. Simulated output power *PW* with various wind speeds *V*.

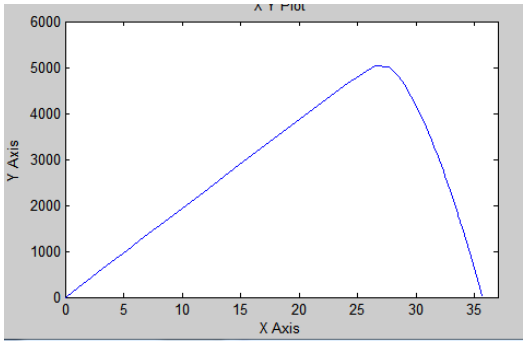

Fig.8 Simulated output power *P*PV versus output voltage *V*PV of the solar cell with constant illumination intensity 1 kW/m2

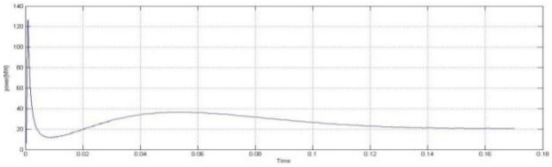

Fig.9 Simulation results of required power (ΔP)

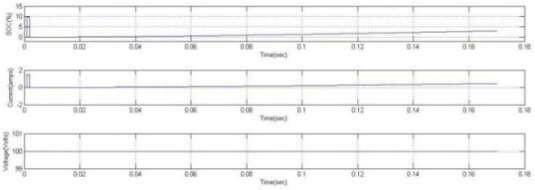

Fig.10 Simulation results of battery SOC

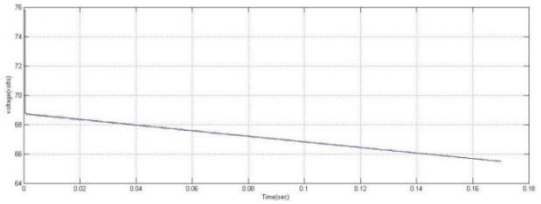

Fig .11 Simulation results of ultra capacitor

This study simulated with constant discharge of 5 A for validation and observation of SOC variation and ultar capacitor are shown in Fig10,11. The battery voltage is easy to measure and implement in the circuit. From the simulated results, we can see the nonlinearity between voltage and SOC of the Li-ion battery

ISSN (Online) 2321 – 2004
ISSN (Print) 2321 – 5526

INTERNATIONAL JOURNAL OF INNOVATIVE RESEARCH IN ELECTRICAL, ELECTRONICS, INSTRUMENTATION AND CONTROL ENGINEERING
Vol. 2, Issue 8, August 2014

VI. CONCLUSSION

This paper shows the operation, analysis and implementation of fuzzy logic control to achieve better performance of the hybrid energy management of Dc micro grid. From the simulation results, the system achieves power balance, and the hybrid combination of battery and ultra capacitor, SOC maintains the desired range for extension of battery life by using the control rules for a dc microgrid. These fuzzy logic rules can be included in the intelligent microgrid management system. The management system takes advantage of the design to control microgrid with power balance, and achieves optimal power control of the dc microgrid system.

REFERENCES

[1] H. Rongxian, L. Zhiwen, C. Yaoming, W. Fu, and R. Guoguang, "DC micro-grid simulation test platform," in Proc. 9thTaiwan Power Electron. Conf., 2010, pp. 1361–1366.
[2] S. Morozumi, "Micro-grid demonstration projects in Japan," in Proc. IEEE Power Convers. Conf., Apr. 2007, pp. 635–642.
[3] Y. Uno, G. Fujita, R. Yokoyama, M. Matubara, T. Toyoshima, and T. Tsukui, "Evaluation of micro-grid supply and demand stability for different interconnections," in Proc. Power Energy Conf., 2006, pp. 611– 616.
[4] Experience in Developing and Promoting 400 V DC Datacenter Power, T. V. Aldridge, Director, Energy Systems Research Lab, Intel Corporate Technology Group, Green Building Power Forum, Jun. 2009.
[5] Maximizing Overall Energy Efficiency in Data Centres, S. Lidstrom, CTO, Netpower Labs AB, Green Building Power Forum, Jun. 2009.
[6] Renewable Energy & Data Centers, J. Pouchet, Director Energy Initiatives, Emerson Network Power., Green Building Power Forum, Jun. 2009.
[7] Development of Higher Voltage Direct Current Power Feeding System in Data Centers, K. Asakura, NTT Energy/Environment, Green Building Power Forum, Dec. 2010.
[8] Specifications for 400 V DC Power Supplies and Facility Equipment, D. Symanski, Sr. Program Manager, Electric Power Research Institute, Keiichi Hirose, NTT Facilities, and Brian Fortenberry, Program Manager, Electric Power Research Institute, Green Building Power Forum, Jan. 2010.
[9] Development of a DC Power Inlet Connector for 400 V DC IT Equipment, B. Davies, Director of Engineering, Anderson Power Products, Inc. Green Building Power Forum, Jan. 2010.
[10] Development of Socket-outlet Bar and Power Plug for 400 V Direct Current Feeding System, T. Yuba, R&D Manager, Fujitsu Components Ltd. Green Building Power Forum, Jan. 2010.
[11] Power Inlet Connector for 380 V DC Data Center, B. Davies, Anderson Power Products, Green Building Power Forum, Dec. 2010.
[12] Intel Lab's New Mexico Energy System Research Center 380 V DC Microgrid Testbed, G. Allee, Intel Labs, Green Building Power Forum, Dec. 2010.
[13] International Standardization of DC Power, K. Hirose, NTT Facilities, Green Building Power Forum, Dec. 2010.

BIOGRAPHIES

JARINA BEGUM has completed B.Tech in Electrical & Electronics Engineering in 2006 from Dr.V.R.K women's college of Engineering, Hyderabad, Affiliated to Jawaharlal Nehru Technological University (JNTUH), Hyderabad, India. She is pursuing M.Tech from Aurora's Research& Technological Institute, Warangal, and Affliated to Jawaharlal Nehru Technological University (JNTUH), Hyderabad, India.Presently working. as Assistant Professor in Ganapathy Engineering College, Warangal, Affliated To Jawaharlal Nehru Technological University (JNTUH), Hyderabad.

CH.SAMPATH KUMAR has completed his B.Tech Electrical& Electronics Engineering in 2006 from Jawaharlal Nehru Technological University, (JNTUH), Hyderabad, India and M.Tech Control Systems in 2010 from Jawaharlal Nehru Technological University (JNTUH), Hyderabad, India. He is currently working as a Associate Professor in the department of Electrical & Electronics Engineering and project Coordinator of M.Tech Control Systems and also Incharge of Examination Department in Aurora's Research & Technological Institute, Warangal, India. He his having eight years of teaching experience.

SHAIK KHAMURUDDIN has completed his B.Tech Electrical & Electronics Engineering in 2006 from JNTUH University, A.P, India and M.Tech Power Systems with Emphasis on High Voltage Engineering in 2009 and presently he is pursuing his PH.D and working as Associate Professor and Head of EEE department at Aurora's Research & Technological Institute, Warangal, Andhra Pradesh, India. He his having total teaching experience of 08 years and his interests are in the areas of power system, power electronics and high voltage engineering.